Monthly Notices
of the
ROYAL ASTRONOMICAL SOCIETY

Mon. Not. R. Astron. Soc. **424,** 1132–1148 (2012) doi:10.1111/j.1365-2966.2012.21289.x

The anticentre old open clusters Berkeley 27, Berkeley 34 and Berkeley 36: new additions to the BOCCE project⋆

P. Donati,[1,2]† A. Bragaglia,[2] M. Cignoni,[1,2] G. Cocozza[2] and M. Tosi[2]

[1]*Dipartimento di Astronomia, via Ranzani 1, 40127 Bologna, Italy*
[2]*INAF-Osservatorio Astronomico di Bologna, via Ranzani 1, 40127 Bologna, Italy*

Accepted 2012 May 10. Received 2012 May 10; in original form 2012 April 16

ABSTRACT

In this paper, we present the investigation of the evolutionary status of three open clusters: Berkeley 27, Berkeley 34 and Berkeley 36, all located in the Galactic anticentre direction. All of them were observed with SUperb Seeing Imager 2 at the New Technology Telescope using the Bessel B, V and I filters. The cluster parameters have been obtained using the synthetic colour–magnitude diagram (CMD) method, i.e. the direct comparison of the observational CMDs with a library of synthetic CMDs generated with different evolutionary sets (Padova, FRANEC and FST). This analysis shows that Berkeley 27 has an age between 1.5 and 1.7 Gyr, a reddening $E(B-V)$ in the range 0.40–0.50 and a distance modulus $(m-M)_0$ between 13.1 and 13.3; Berkeley 34 is older with an age in the range 2.1–2.5 Gyr, $E(B-V)$ between 0.57 and 0.64 and $(m-M)_0$ between 14.1 and 14.3; Berkeley 36, with an age between 7.0 and 7.5 Gyr, has a reddening of $E(B-V) \sim 0.50$ and a distance modulus $(m-M)_0$ between 13.1 and 13.2. For all the clusters, our analysis suggests a subsolar metallicity in accord with their position in the outer Galactic disc.

Key words: Hertzsprung–Russell and colour–magnitude diagrams – Galaxy: disc – open clusters and associations: general – open clusters and associations: individual: Berkeley 27 – open clusters and associations: individual: Berkeley 34 – open clusters and associations: individual: Berkeley 36.

1 INTRODUCTION

This paper is part of the Bologna Open Clusters Chemical Evolution (BOCCE) project, described in detail by Bragaglia & Tosi (2006). The aim of the project is to precisely and homogeneously derive the fundamental properties of a large, significant sample of open clusters (OCs). OCs are among the best tracers of the properties of the Galaxy (e.g. Friel 1995). They can be used to get insight on the formation and evolution of the Galactic disc(s), the final goal of the BOCCE project. We have already published results based on photometry for 26 OCs (see Bragaglia & Tosi 2006; Cignoni et al. 2011, and references therein), concentrating on the old ones, the most important to study the early epochs of the Galactic discs.

The three clusters examined in this paper are Berkeley 27 (also known as Biurakan 11 and hereafter Be 27 with Galactic coordinates $l = 207.^{\circ}8, b = 2.^{\circ}6$), Berkeley 34 (also known as Biurakan 13 and hereafter Be 34, $l = 214.^{\circ}2, b = 1.^{\circ}9$) and Berkeley 36 (Be 36 hereafter, $l = 227.^{\circ}5, b = -0.^{\circ}6$). They are all located in the anticentre direction, very close to the Galactic plane and have an age older than 1 Gyr. They were selected because, based on literature studies, they all lie beyond a Galactocentric distance of 10 kpc; hence, they can be useful to understand the properties of the outer disc. In particular, they are located in the region where the radial metallicity distribution changes its slope and where more clusters should be studied to better understand why this happens (see e.g. Sestito et al. 2008; Friel, Jacobson & Pilachowski 2010; Andreuzzi et al. 2011; Lépine et al. 2011). These OCs have already been studied to different degrees in the past: the resulting parameters sometimes agree with each other and sometimes not. We present here their *BVI* photometry, used to improve upon previous determinations of their parameters using the colour–magnitude diagram (CMD) synthetic method, as done throughout the BOCCE series.

All three clusters have been studied by Hasegawa et al. (2004) as part of a survey of 14 anticentre clusters; they obtained *BVI* photometry with a 0.65-m telescope. Be 27 has also been studied by Carraro & Costa (2007) using *VI* photometry acquired at a 0.9-m telescope. Be 34 and Be 36 have also been observed by Ortolani et al. (2005) at a 3.5-m telescope using the *BV* filters. In all the three papers, the cluster parameters have been derived using isochrone fitting.

⋆ This work is based on data collected at the European Southern Observatory (ESO) telescopes under programme 076.D-0119.

†E-mail: paolo.donati4@unibo.it

Concerning Be 27, Hasegawa et al. (2004) find a cluster age of 2.0 Gyr, a mean Galactic reddening of $E(V-I) = 0.30$ [or $E(B-V) = 0.24$], a distance modulus of $(m-M)_0 = 14.25$ and a metallicity of $Z = 0.03$; however, according to them, some ambiguity in the photometric calibration could have hampered the interpretation of the data. Carraro & Costa (2007) confirm a cluster age of 2.0 Gyr, but prefer a higher reddening of $E(B-V) = 0.35$ and a distance modulus of $(m-M)_0 = 14.30$; they used the Padova tracks with solar metal abundance ($Z = 0.019$). The cluster lacks a clear red giant branch (RGB) and clump, which makes the analysis of the cluster more uncertain.

For Be 34, Hasegawa et al. (2004) find a cluster age of 2.8 Gyr, a mean reddening of $E(V-I) = 0.60$ [i.e. $E(B-V) = 0.48$], a distance modulus of $(m-M)_0 = 15.80$ and a metallicity of $Z = 0.019$. Ortolani et al. (2005) suggest two different interpretations with two different metallicities: 2.3 Gyr, $E(B-V) = 0.30$ and $(m-M)_0 = 15.4$ for Padova isochrones with $Z = 0.019$; 2.3 Gyr, $E(B-V) = 0.41$ and $(m-M)_0 = 15.62$ for $Z = 0.008$. Be 34 does not have a clear clump either and the contamination of field stars is important, conditions that put more uncertainties on the estimation of the cluster parameters.

In the case of Be 36, Hasegawa et al. (2004) find a cluster age of 3.4 Gyr, a reddening of $E(V-I) = 0.55$ [i.e. $E(B-V) = 0.44$], a distance modulus of $(m-M)_0 = 15.30$ and a metallicity of $Z = 0.019$. They could not firmly define the clump as the cluster showed a blurred and heavily contaminated CMD; therefore, they adopted the solution that could fit appropriately the main sequence (MS) and the RGB. Ortolani et al. (2005) present two different cluster parameter estimations using the Padova tracks with $Z = 0.019$ and 0.008. For the solar metallicity they find a cluster age of 4 Gyr, $E(B-V) = 0.25$ and $(m-M)_0 = 14.70$; for the subsolar metallicity they find $E(B-V) = 0.36$, $(m-M)_0 = 14.85$ and an age of 4 Gyr. They chose different MS turn-off (TO) and red clump (RC) levels with respect to Hasegawa et al. (2004), and this can explain the differences in the results obtained.

This paper is organized as follows. Observations and the resulting CMDs are presented in Section 2; the estimation of the cluster centre is given in Section 3; the derivations of their age, distance, reddening and metallicity using comparison to synthetic CMDs are given in Section 4. Discussion and summary can be found in Section 5.

2 THE DATA

2.1 Observations

The three clusters were observed in service mode at the ESO 3.58-m New Technology Telescope (NTT) of the La Silla Observatory (Chile) with the instrument SUperb Seeing Imager 2 (SUSI2) in 2005 and 2006. The instrument was composed by a mosaic of two EEV CCDs (2048 × 4096 pixel) placed in a row. The field of view (FoV) of SUSI2 is equivalent to 5.5 × 5.5 arcmin^2, with a pixel scale of 0.085 arcsec pixel^{-1}; for these observations the instrument was set in the 2 × 2 binned mode (pixel scale 0.161 arcsec). The data were collected with the *B*, *V* and *I* Bessel filters. The clusters were positioned at the geometric centre of the mosaic with the rotator in the default position; two of them were also observed with the instrument rotated 90° clockwise in order to recover stars falling in the mosaic gap. Digitized Sky Survey (DSS) images of the SUSI2 FoV for the pointings of Be 27, Be 34 and Be 36 are shown in Figs 1–3. The observations logbook for the three clusters is presented in Table 1. Comparison fields were also observed for decontamination purposes, located 30 arcmin away from the cluster centre (see Table 1). The seeing was below 1.5 arcsec for all images and below 1 arcsec for many. For each cluster, observations in photometric conditions were obtained which allowed a proper calibration using the photometric standard fields SA98, SA101-262, PG0918 and RU152 (Landolt 1992).

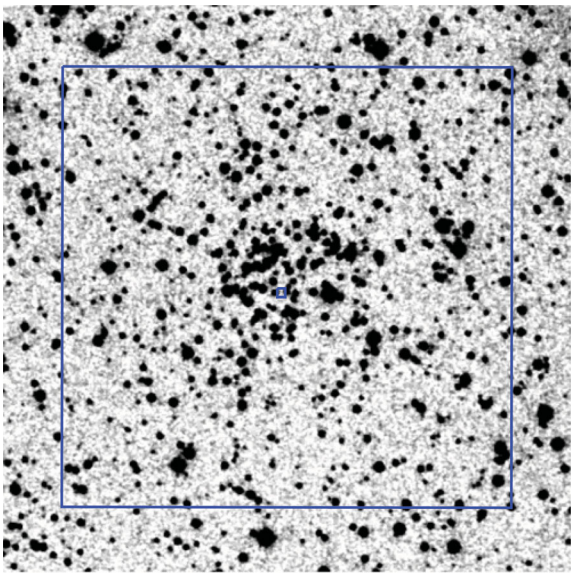

Figure 1. DSS image of the FoV centred on Be 27. The box is the composite FoV of SUSI2 obtained with the rotator in different positions: only the stars inside the smaller central box fell in the mosaic gap.

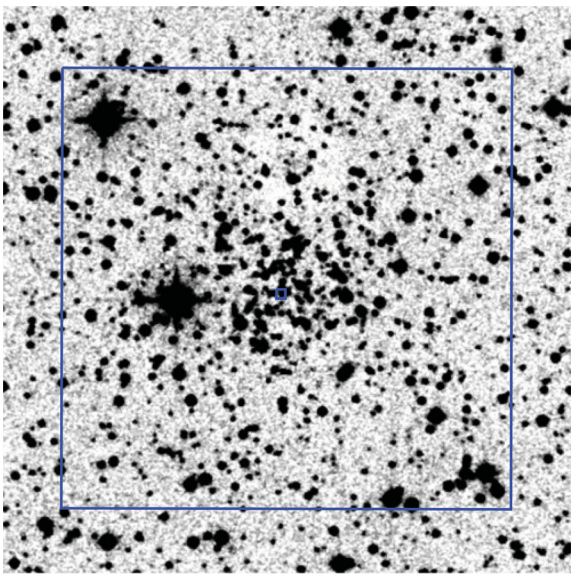

Figure 2. Same as Fig. 1, but for Be 34.

2.2 Data reduction

Bias and flat-field corrections were done using a standard analysis with IRAF.[1]

[1] IRAF is the Image Reduction and Analysis Facility, a general purpose software system for the reduction and analysis of astronomical data. IRAF is written and supported by the IRAF programming group at the National Optical Astronomy Observatories (NOAO) in Tucson, Arizona.

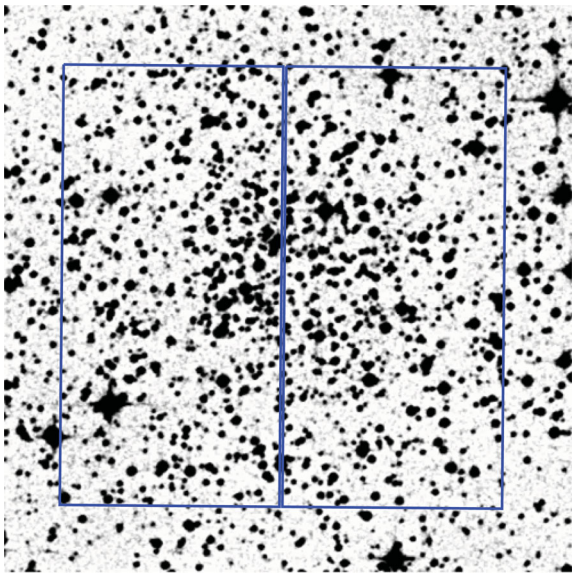

Figure 3. Same as Fig. 1, but for Be 36. In this case only the default orientation was used and the FoV has a gap apparent in the figure.

The source detection and relative photometry were performed independently on each *B*, *V* and *I* image, using the point spread function (PSF) fitting code DAOPHOTII/ALLSTAR (Stetson 1987, 1994). For each frame a sample (20–70) of isolated and bright stars was selected to compute the PSF. The profile-fitting algorithm was imposed to determine a spatially variable PSF to include a quadratic dependence on the *x* and *y* coordinates in order to minimize geometrical distortion biases. Different exposure times let us recover the efficiently bright and faint stars.

The next step was to remove any systematic difference between the magnitude scales of all the frames. The stars in each frame were first matched to the ones taken in photometric conditions using DAOMATCH and DAOMASTER. Then the average and the standard errors of the mean of independent measures obtained from different images were adopted as the final values of the instrumental magnitude and uncertainty.

About 20 standard areas (∼6 per filter) were observed during each photometric night and the magnitude of the standard stars was measured. Three sets of calibration equations were derived, as the targets were observed in different nights. The results are reported in Table 2.

As the photometry of the standard stars was computed using aperture photometry, the instrumental magnitudes of the scientific targets were corrected to match the standard Johnson–Cousins system and then calibrated. Two different calibration equations were derived for the *V* magnitude: one using the $(B-V)$ colour index and the other using the $(V-I)$ colour index. The difference between the two calibrations is, on average, well below one-hundredth of a

Table 2. Calibration equations. *B*, *V* and *I* are the magnitudes in the standard Johnson–Cousins system while *b*, *v* and *i* are the instrumental magnitudes.

Cluster	Date	Equation	rms
Be 27	2006 February 19	$B = b - 0.143(b-v) + 0.275$	0.017
		$V = v - 0.016(b-v) + 0.562$	0.024
		$V = v - 0.019(v-i) + 0.540$	0.023
		$I = i - 0.016(v-i) - 0.450$	0.019
Be 34	2006 February 24	$B = b - 0.125(b-v) + 0.312$	0.023
		$V = v - 0.010(b-v) + 0.620$	0.023
		$V = v - 0.014(v-i) + 0.602$	0.019
		$I = i - 0.035(v-i) - 0.376$	0.022
Be 36	2006 February 25	$B = b - 0.129(b-v) + 0.318$	0.015
		$V = v - 0.016(b-v) + 0.631$	0.019
		$V = v - 0.015(v-i) + 0.606$	0.018
		$I = i - 0.024(v-i) - 0.367$	0.018

Table 1. Log of observations.

Cluster	RA (h m s) (J2000)	Dec. (° ′ ″) (J2000)	Date	Rot[a]	*B* Exp. time (s)	*V* Exp. time (s)	*I* Exp. time (s)
Be 27	6 51 21	+05 46 00	2005 November 29	a	10, 44, 540	5, 270	5, 270
				b	10, 540	5, 270	5, 270
			2006 February 19	a	50, 100	50, 50	50, 50
				b	100	50	50
Be 27 ext	6 51 21	+05 18 00	2005 November 29	a	2 × 10, 560	5, 280	5, 280
			2006 February 19	a	100	50	50
Be 34	7 00 23	−00 14 11	2005 November 29	b	10, 103, 540	5, 270	5, 270
			2006 January 26	a	10, 540	2 × 5, 270	2 × 5, 270
				b	4 × 10, 2 × 540	4 × 5, 2 × 270	4 × 5, 2 × 270
			2006 February 24	a	100	50	50
				b	100	50	50
Be 34 ext	7 00 23	−00 50 11	2005 November 29	a	10, 77, 560	5, 280	5, 280
			2006 February 24	a	100	50	50
Be 36	7 16 24	−13 11 50	2006 January 26	a	10, 540	5, 270	2 × 5, 270
			2006 February 25	a	100	50	50
			2006 March 20	a	100	50	50
Be 36 ext	7 16 24	−13 42 00	2006 January 26	a	10, 560	5, 280	5, 280
			2006 February 25	a	100	50	50
			2006 March 20	a	100	50	50

[a]Angle of the rotator: 'a' means default position and 'b' means 90° clockwise.

Table 3. Completeness of the photometry for the three clusters.

Mag	Compl *B*	Compl *V* Be 27	Compl *I*	Compl *B*	Compl *V* Be 34	Compl *I*	Compl *B*	Compl *V* Be 36	Compl *I*
16.0	100 ± 6	99 ± 5	100 ± 4	100 ± 6	100 ± 6	99 ± 5	100 ± 6	99 ± 5	99 ± 4
16.5	99 ± 6	98 ± 3	100 ± 3	100 ± 5	100 ± 5	99 ± 4	100 ± 5	98 ± 5	98 ± 4
17.0	99 ± 4	99 ± 3	99 ± 3	100 ± 5	98 ± 4	98 ± 3	99 ± 5	99 ± 4	98 ± 3
17.5	99 ± 3	98 ± 2	98 ± 3	98 ± 4	98 ± 4	97 ± 3	99 ± 5	99 ± 4	98 ± 2
18.0	98 ± 3	99 ± 2	98 ± 2	99 ± 4	98 ± 3	97 ± 2	100 ± 4	98 ± 3	97 ± 2
18.5	98 ± 2	97 ± 2	96 ± 2	98 ± 3	98 ± 3	96 ± 2	98 ± 4	97 ± 2	98 ± 2
19.0	98 ± 2	97 ± 2	96 ± 2	99 ± 3	97 ± 2	94 ± 2	97 ± 3	98 ± 2	96 ± 2
19.5	97 ± 2	96 ± 2	96 ± 2	98 ± 2	97 ± 2	94 ± 2	98 ± 2	97 ± 2	95 ± 2
20.0	98 ± 2	96 ± 2	93 ± 2	97 ± 2	96 ± 2	90 ± 2	98 ± 2	96 ± 2	94 ± 2
20.5	96 ± 2	95 ± 2	88 ± 2	96 ± 2	95 ± 2	74 ± 2	96 ± 2	95 ± 2	88 ± 2
21.0	95 ± 2	93 ± 2	80 ± 2	95 ± 2	92 ± 2	38 ± 3	96 ± 2	94 ± 2	75 ± 2
21.5	94 ± 2	88 ± 2	59 ± 2	92 ± 2	87 ± 2	5 ± 7	94 ± 2	89 ± 2	42 ± 3
22.0	88 ± 2	78 ± 2	36 ± 3	72 ± 2	50 ± 3	0	84 ± 2	71 ± 2	7 ± 6
22.5	74 ± 2	59 ± 2	13 ± 5	17 ± 4	8 ± 6	0	34 ± 3	23 ± 3	0
23.0	52 ± 2	35 ± 2	2 ± 11	3 ± 10	1 ± 18	0	4 ± 8	2 ± 11	0

magnitude with a small dispersion and a very shallow dependence on colour.

The Guide Star Catalogue 2.3 was used to find an accurate astrometric solution to transform the instrumental pixel positions into J2000 celestial coordinates. More than 200 stars were used for each frame as astrometric standards and the final transformations, obtained with the code CATAXCORR,[2] have an rms scatter less than 0.2 arcsec in both right ascension (RA) and declination (Dec.).

The final step of the data reduction process consisted of recovering the completeness level of the photometry. The procedure is the classical one consisting of an extensive artificial stars experiment, already used in our previous works (see e.g. Bellazzini et al. 2002, for a description). About 50 000 stars have been artificially added and uniformly distributed on the deepest frames in groups of about 120 stars at a time, to avoid changing the actual crowding conditions. For each iteration of the artificial stars' experiment the frames were reduced using the same reduction process described above. The fraction of recovered stars at different magnitude levels represents the completeness of our photometry; values are presented in Table 3.

2.3 Colour–magnitude diagrams

The resulting CMDs for the cluster stars and the comparison field stars are shown in Fig. 4 (V, $B-V$ plane) and Fig. 5 (V, $V-I$ plane). Error bars indicate the global photometric error that takes into account the instrumental error and the uncertainties on the calibration procedures. They range from about 0.03 mag at the bright limit to less than 0.1 mag around $V = 24$. The main evolutionary phases of the three OCs are visible despite the important field contamination. In particular, the MS is easily recognizable although its broad shape does not help in defining its features. The detailed analysis of the CMD's morphology is described in Section 4.

2.4 Comparison with previous data

As mentioned in Section 1, Be 27, Be 34 and Be 36 were previously observed by various authors. The web data base for OCs, WEBDA,[3] was exploited to obtain literature data. In particular, Be 27 was studied by Hasegawa et al. (2004) and Carraro & Costa (2007), and Be 34 and Be 36 by Hasegawa et al. (2004) and Ortolani et al. (2005). The analysis described in Hasegawa et al. (2004) uses B, V and I photometry but they made public through WEBDA only data with $V < 18$. Furthermore, for Be 27 they declare to have problems of photometric calibration. Therefore, we decided to show a comparison only with the data from Carraro & Costa (2007) which contains V and I photometry for Be 27 and with the data from Ortolani et al. (2005) that has B and V photometry for Be 34 and Be 36. In Figs 6–8 the comparisons of the photometries are shown together with the literature CMDs.

Concerning Be 27 (Fig. 6), the difference in the V filter is, on average, -0.04 mag with a very shallow slope for bright stars. The difference in the I filter is a bit larger, about -0.07 mag, leading to an average difference in $(V-I)$ colour of $+0.03$. We cannot tell if these small differences are due to our photometry or theirs since there are no reliable data in the literature for this cluster. Moreover, it is not possible to solve the issue with general considerations about our ability to calibrate the photometry to the standard system because our OCs were observed in different nights.

For Be 34 (Fig. 7) and Be 36 (Fig. 8) the comparison of V gives an average difference of -0.085 and -0.056 mag, respectively, while for the B photometry we find a difference of $+0.024$ and $+0.174$ mag. For the former OC the difference in B is small but becomes important in V, leading to a difference in $(B-V)$ of $+0.11$ mag. In the case of Be 36 the disagreement in B is quite significant and we obtain an average difference in $(B-V)$ of $+0.23$ mag. The explanation of such differences is not straightforward as it is not possible to definitely distinguish if they are due to our photometry or theirs. Both our targets and theirs were observed in two different nights with no significant difference in the calibration parameters

[2] CATAXCORR was developed by Paolo Montegriffo at INAF – Osservatorio Astronomico di Bologna.

[3] web version of the data base known as BDA (Base Donńees Amas) maintained by Ernst Paunzen and Christian Stütz at http://www.univie.ac.at/webda/

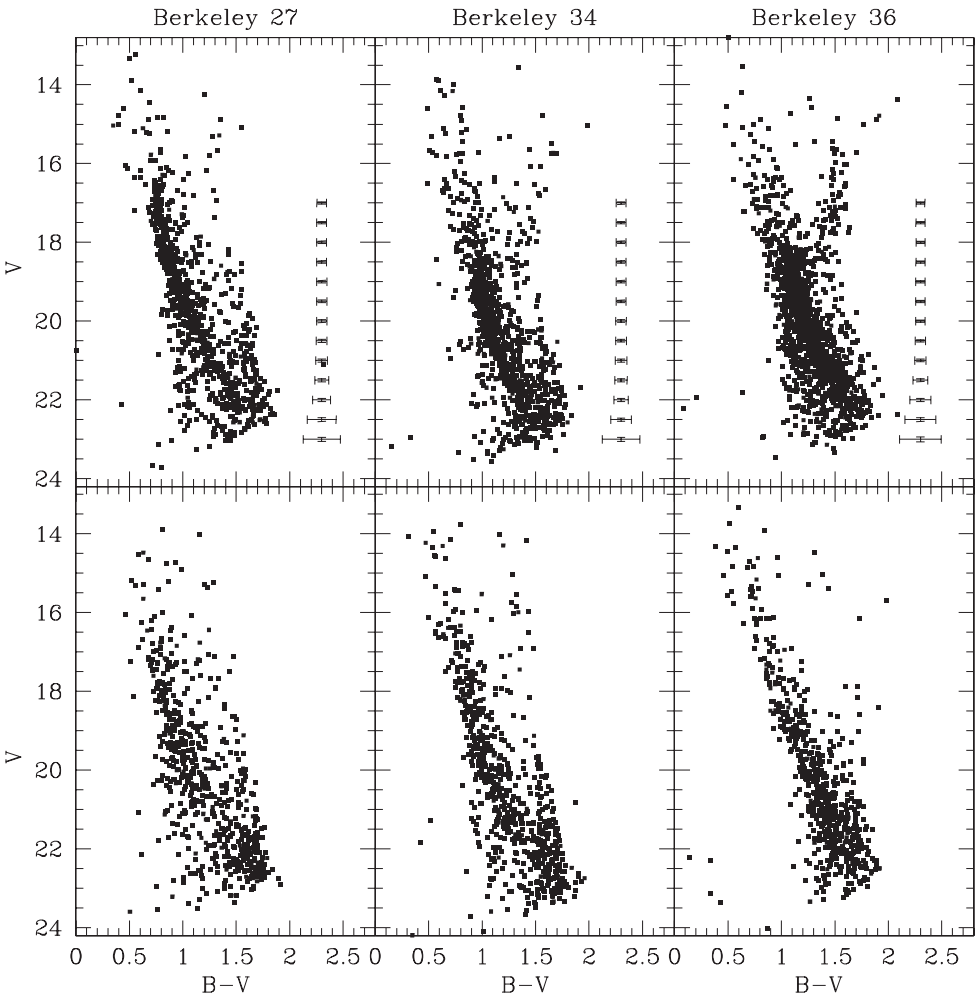

Figure 4. Upper panels: CMDs of Be 27, Be 34 and Be 36 showing V versus $(B - V)$. Lower panels: CMDs of the corresponding comparison field. Global photometric errors are shown on the right-hand side of the cluster CMDs.

obtained for the two nights. Furthermore, we had some problems in attempting the cross-correlation of our astrometrized catalogues with the pixel-coordinate ones of Ortolani et al. (2005). We could find a good match only after dividing the whole literature catalogues into two halves: one with all the stars with x coordinates smaller than 1025 and the other one with x coordinates larger than 1025. This problem is probably due to the geometrical distortion in the alignment of the two CCDs' pixel coordinates given by Ortolani et al. (2005). In addition, we noted that for Be 36 the original data file available through WEBDA (the same as we downloaded from the VizieR portal[4]) contains differences with respect to the CMD shown in Ortolani et al. (2005) and the plot facilities of the WEBDA itself. Therefore, we chose to show in Fig. 8 only the CMD of the stars in common with our catalogue and we assumed that our photometry is on the standard system in the following analysis.

3 CLUSTER CENTRE

Occasionally, the cluster centre indicated in the WEBDA (taken from the Dias et al. 2002 catalogue and updates) is offset from the true one by a few arcminutes; therefore, we check if this is the case for the three OCs. For each object we computed its centre as the barycentre of the stars' spatial distribution on the basis of a simple statistical approach. The three clusters are all distant objects, so their apparent diameter is relatively small, giving us the chance to distinguish the central part even with the small FoV of SUSI2. From the Dias et al. (2002) catalogue we know that the apparent diameter of the clusters (based on visual inspection) is about 2 arcmin for Be 34 and 5 arcmin for Be 36, while for Be 27 the recent study by Carraro & Costa (2007) indicates a cluster radius of 3 arcmin. This means that two of our OCs are fully contained in the SUSI2 FoV, while Be 27 is slightly larger.

To identify the centre, first we restricted our analysis only to stars that belong to the upper part of the CMDs (selecting those with $V \leq 22$) to have a smaller sample of objects strongly dominated by cluster stars with a relative small contamination of field stars. Then we performed a spatial selection: we computed the smallest intervals in coordinates RA and Dec. that contain 70 per cent of stars and, with this smaller group, we iterated the computation to define a spatial region used to refine our analysis. The cluster centre is then computed as the barycentre of the final group of stars.

The guidelines adopted for the spatial selection are set heuristically, aiming at taking into account not only the clustering level of the stars (which dominates on small scales) but also the sparse nature and asymmetric distribution of objects in OCs (which dominates on large scales). The constraints on the algorithm seemed

[4] http://vizier.u-strasbg.fr/viz-bin/VizieR

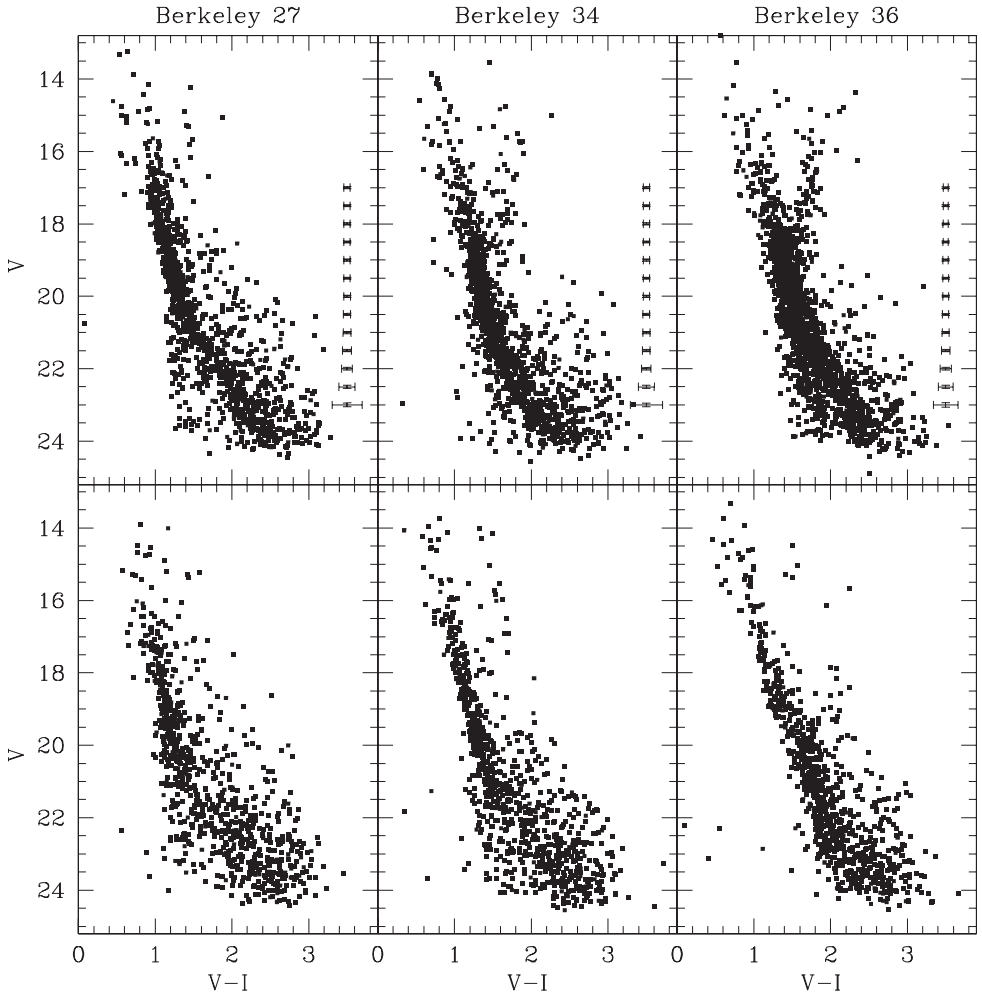

Figure 5. Same as Fig. 4, but for V versus $(V - I)$.

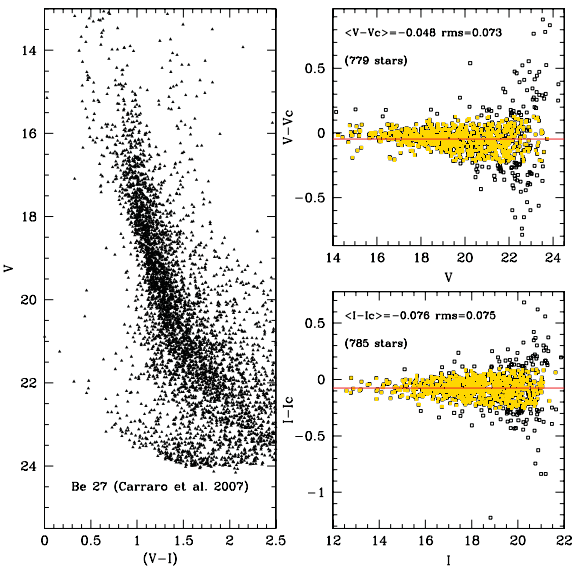

Figure 6. Left-hand panel: CMD of Be 27 by Carraro & Costa (2007). Right-hand panel: differences between our photometry and theirs in V (upper panel) and I (lower panel). The points in the plots are the photometric data for all the stars in common; filled ones are stars used to compute the mean differences (within 2σ from the average).

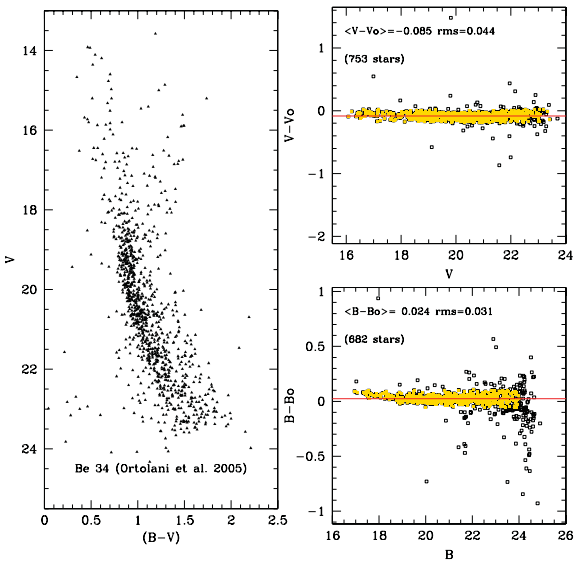

Figure 7. Left-hand panel: CMD of Be 34 by Ortolani et al. (2005). Right-hand panel: comparison with our data for V (upper panel) and B (lower panel) magnitudes (see Fig. 6).

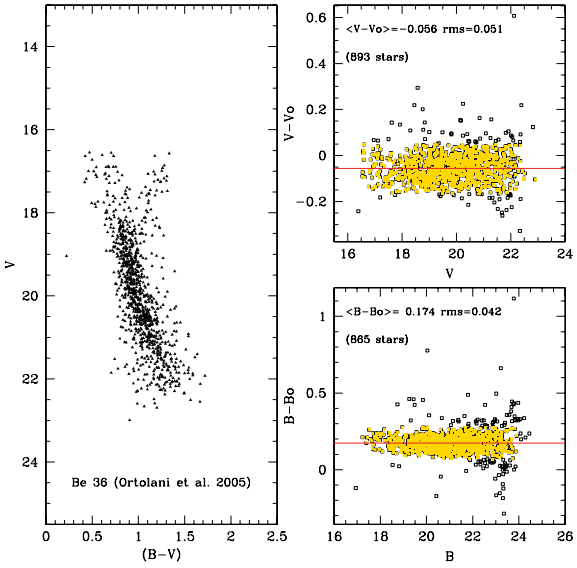

Figure 8. Left-hand panel: CMD of Be 36 by Ortolani et al. (2005) of the stars in common with our catalogue. Right-hand panel: comparison with our data (see previous figure).

Table 4. J2000 RA and Dec. coordinates for the three clusters. The second and third columns are the computed coordinates of the centre. The last two columns contain the previous determinations of the centre.

Cluster	Centre		Previous determination[a]	
	RA (h m s)	Dec. (° ′ ″)	RA (h m s)	Dec. (° ′ ″)
Be 27	06 51 21	+05 46 07	06 51 18	+05 46 00
Be 34	07 00 23	−00 13 56	07 00 24	−00 15 00
Be 36	07 16 24	−13 11 35	07 16 06	−13 06 00

[a]Source: WEBDA.

to have a good trade-off, confirmed by the small dispersion of the results with respect to different magnitude selections (7 arcsec for RA and 2 arcsec for Dec.).

The results, which are the average of different selections of magnitude, are shown in Table 4. They are slightly different from the ones available in the literature, especially for Be 36.

4 CLUSTER PARAMETERS USING SYNTHETIC COLOUR–MAGNITUDE DIAGRAMS

The estimations of age, metallicity, distance, mean Galactic reddening and binary fraction have been obtained comparing the observational CMDs with a library of synthetic ones, built using synthetic stellar populations (see e.g. Tosi, Bragaglia & Cignoni 2007; Cignoni et al. 2011). Different sets of evolutionary tracks[5] have been used to obtain the synthetic CMDs via Monte Carlo simulations. The comparison between synthetic and observed CMDs is based on the CMD morphology and number counts. The best-fitting solution is chosen as the one that can best reproduce some age-sensitive indicators, such as the luminosity level of the MS reddest point ('red hook', RH), the RC and the main-sequence termination point (MSTP, evaluated as the maximum luminosity reached after the overall contraction, OvC, and before the runaway to the red), the luminosity at the base of the RGB, the RGB inclination and colour, and the RC colour. The last two were used as secondary age indicators as colour properties are more affected by theoretical uncertainties, like colour transformations and the superadiabatic convection, while luminosity constraints are more reliable.

The most valuable age indicator is the TO point, that is the bluest point after the OvC and the RC luminosity; however, at least in the case of OCs, these phases may be very poorly populated, and identifying them is not a trivial game, especially if a strong field star's contamination is present.

In order to make a meaningful comparison, the synthetic CMDs are made taking into account the photometric error, the completeness level of the photometry and the stellar density contrast of the OC's population with respect to the population of the comparison field. The synthetic CMDs are combined with stars picked from an equal area of the comparison field to take the contamination into account.

As done in Cignoni et al. (2011), we first evaluate the parameters that do not depend on the evolutionary model analysis, such as the binary fraction and the differential reddening. The binary fraction is estimated from the information on colour and magnitude of the cluster stars and then fine-tuned, together with the differential reddening parameter, in order to match the MS width. In the analysis described in the next paragraphs the adopted differential reddening is considered as an upper limit and added as a random positive constant to the mean Galactic reddening. The luminosity of the MSTP and the RC are effectively used to constrain the age. The estimated luminosity of the base of the RGB (BRGB), the RGB inclination and colour, and the RC colour are used to select the best fit to the observational CMDs in order to estimate the mean Galactic reddening $E(B-V)$ and the observed distance modulus $(m-M)_0$, and to fine-tune the metallicity. The best estimate of the mean Galactic reddening is defined when the bluest upper part of the synthetic CMD MS matches the corresponding part of the observed CMD MS; the observed distance modulus is identified when the MSTP level and colour are reproduced in the synthetic CMD. The information of the complete *BVI* photometry to constrain the metallicity (see Tosi et al. 2007) and reduce the parameter space of our analysis was taken into account: the best metallicity is defined when it is possible to reproduce at the same time the observed $B-V$ and $V-I$ CMDs with the synthetic ones for appropriate distance modulus, reddening and age. To deal with $(B-V)$ and $(V-I)$ colours we adopted the normal extinction law where $E(V-I) = 1.25 \times E(B-V) \times [1 + 0.06 \times (B-V)_0 + 0.014 \times E(B-V)]$ (Dean, Warren & Cousins 1978).

This procedure relies mostly on the MS fitting and the RC fitting. Hence, the main uncertainties of the results are due to the fact that the MS inclination, RC morphology and luminosity are quite sensitive to the input physics of the model and to the adopted colour transformations, and the uncertainties in defining the RC stars are not negligible for poorly populated clusters, increasing the probability of confusion with RGB and field stars biasing the age determination. In this context the 'best' solution parameters are chosen as the ones that fit most of the visible MS shape and the assumed RC level.

We estimated the errors on the cluster parameters (mean Galactic reddening, distance modulus and cluster age) considering the

[5] The Padova (Bressan et al. 1993), FRANEC (Dominguez et al. 1999) and FST ones (Ventura et al. 1998) of all available metallicities as in all the papers of the BOCCE series.

instrumental photometric error and the uncertainties of the fit analysis. The net effect of the former is an uncertainty on the luminosity level and colour of the indicators adopted. This in particular affects the mean Galactic reddening and the distance modulus estimations as they are directly defined by matching the level and colour of the upper MS and the RH and MSTP indicators of the observed CMDs with the synthetic ones. For the latter we consider the dispersion in the results arising from the fit analysis: OCs offer poor statistics and important age-sensitive indicators, such as the RC locus, are poorly defined; hence there is no unambiguous solution but a range of compatible solutions. Then we select the best-fitting synthetic CMD, and the dispersion of the cluster parameter estimates for different solutions in the error budget is taken into account. The uncertainties are taken to be of the form

$$\sigma^2_{E(B-V)} \sim \sigma^2_{(B-V)} + \sigma^2_{\rm fit},$$

$$\sigma^2_{(m-M)_0} \sim \sigma^2_V + R^2_V \sigma^2_{E(B-V)} + \sigma^2_{\rm fit},$$

$$\sigma^2_{\rm age} \sim \sigma^2_{\rm fit}.$$

The typical photometric error for the reddening is ∼0.04 and that for the distance modulus it is ∼0.1 (we considered the error to be negligible on R_V); the dispersion for the fit analysis depends mainly on the uncertainty on the RC level and on the coarseness

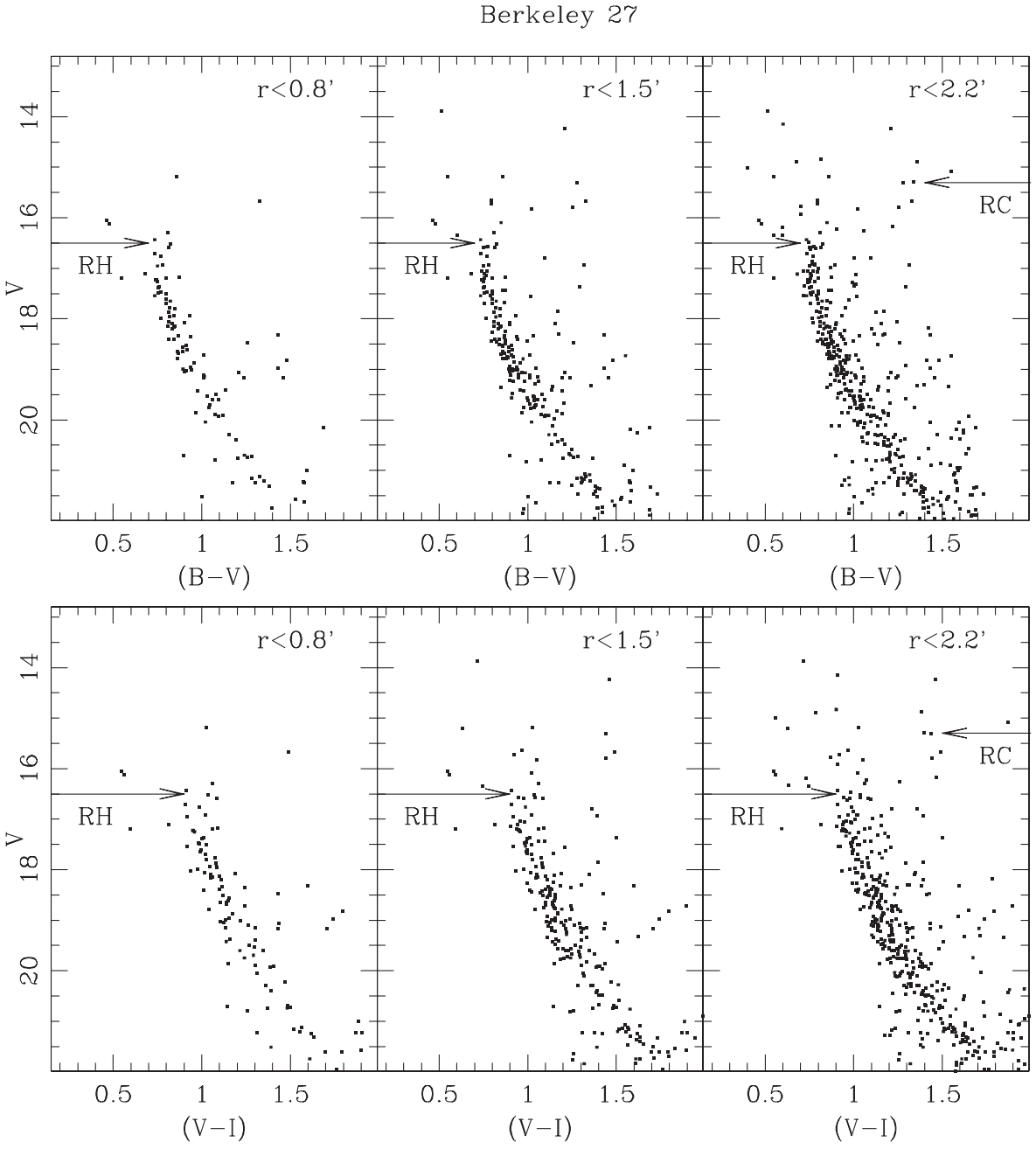

Figure 9. Upper panels show the V versus $(B - V)$ CMDs of Be 27 for different distances r from the cluster centre. Lower panels: the same but for the V versus $(V - I)$ CMDs. In the plots the level of RH (solid arrow on the left) and RC (solid arrow on the right) are also indicated.

of the isochrone grid. It is of the order of ∼0.02 for the reddening, ranges between 0.01 and 0.05 for the distance modulus and about 0.2–1 Gyr for the age.

4.1 Berkeley 27

Be 27 is a poorly populated cluster: the contrast of member stars with the comparison field stars outlines the cluster MS but other evolutionary phases are not easily recognizable. For a more robust analysis we studied the inner part of the cluster which is less contaminated by field interlopers. Fig. 9 shows CMDs for different circular areas around the cluster centre: the left-hand panels are the CMDs for the smallest area (distance from the centre $r < 0.8$ arcmin) and only the MS is clearly visible. We indicate the RH level with a solid arrow on the left; the MS shows a little bend towards the red just below the RH and then reaches its reddest point at $V \sim 16.5$. The two blue stars at $(B - V) \sim 0.45$ and $V \sim 16$ are probably cluster blue straggler stars (very common in OCs, see e.g. Ahumada & Lapasset 2007 for a recent catalogue). The central panels of the same figure show the CMD for stars with a distance from the cluster centre smaller than 1.5 arcmin and the right one for a distance $r < 2.2$ arcmin. Concerning the RC stars there is no firm evidence from the CMDs; we define the most probable RC locus (solid arrow on the right) choosing the two stars at magnitude $V \sim 15.2$ and colour $(B - V) \sim 1.3$–1.4: these stars are close to the centre, hence they are more likely cluster members and have a very small difference both in $B - V$ and $V - I$ colours; in addition, our choice is in agreement with the analysis by Carraro & Costa (2007). The RC stars are very few but still more abundant than the comparison field stars (see CMDs in Fig. 10 for a circular area of $r = 2.2$ arcmin). The uncertainty in defining the magnitude level of the RC directly affects the precision of the age estimate. We use the CMD for $r < 2.2$ arcmin in the further analysis to limit the field contamination.

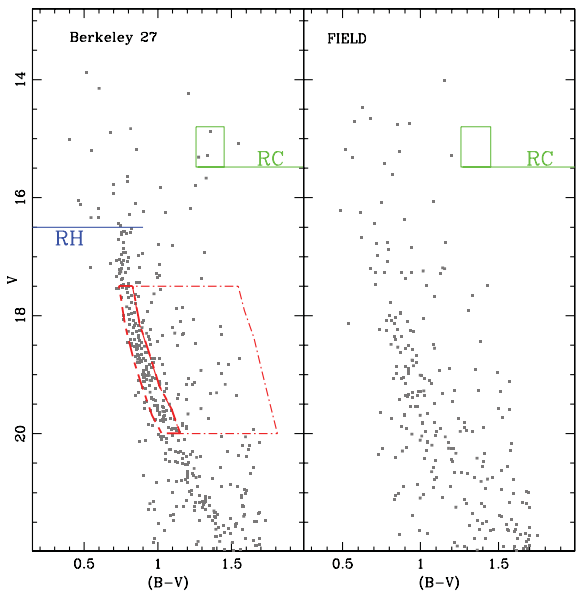

Figure 10. Left-hand panel: CMD of Be 27 for stars falling inside a region of 2.2 arcmin from the cluster centre. We indicate the luminosity level of the RH and the RC. The dotted and the dot–dashed boxes are, respectively, used to estimate the fraction of single and binary stars. Right-hand panel: CMD of the comparison field of an equal area.

The MS appears broader than expected from photometric errors. This is probably due to two factors: one is a large fraction of binaries and the other is the presence of differential reddening. For our simulations we need to assume a differential reddening of $\Delta E(B - V) = 0.05$ mag in addition to the mean Galactic reddening.

A rough estimate of the binary fraction was obtained following the method described in Cignoni et al. (2011): we defined two CMD boxes, one which encloses MS stars and the other redward of the MS in order to cover the binary sequence (see dashed and dot–dashed lines in Fig. 10). To remove the field contamination we subtracted the contribution of field stars falling inside the same CMD boxes of an equal area of the control field. We performed the same computation on regions smaller and larger than 2.2 arcmin, finally ending with an estimate between 20 and 30 per cent. The dispersion on the estimate is mostly due to the spatial fluctuations across the control field. Moreover, these fractions are underestimated: we are missing binaries hosting low-mass star, whose properties are close to those of single stars. However, a mean fraction of 25 per cent appears a reasonable trade-off and will be assumed for all the simulations.

We performed the simulations looking for the best combination of parameters keeping fixed the binary fraction and differential reddening derived above. The interval of confidence for the cluster age turns out between 1.2 and 1.8 Gyr. Concerning the metallicity, we find that all models with solar metallicity cannot fit the stellar population both in $(B - V)$ and $(V - I)$ colours. Therefore, we concentrate our efforts on solutions with $Z < 0.02$.

The FST models with $Z = 0.006$ and 0.01 (overshooting parameter $\eta = 0.2$) fit reasonably well the RH and RC luminosity levels. The synthetic MS is slightly redder than the observed one in the magnitude range $18.5 < V < 20$ mag and this is probably due to the fact that the synthetic MS shape is too curved before the RH point. In terms of cluster parameters $Z = 0.006$ implies a cluster age of 1.5 ± 0.2 Gyr, $E(B - V) = 0.50 \pm 0.04$ and a distance modulus of $(m - M)_0 = 13.20 \pm 0.13$; $Z = 0.01$ implies a cluster age of 1.5 ± 0.2 Gyr, $E(B - V) = 0.44 \pm 0.04$ and a distance modulus of $(m - M)_0 = 13.27 \pm 0.13$. We cannot firmly choose between the two metallicities $Z = 0.006$ and 0.01: from the comparison of $(B - V)$ and $(V - I)$ CMDs with the observed ones we find a good match in both cases. This means that the metallicity estimate suffers more uncertainties, as we cannot obtain a unique and independent evaluation from the *BVI* photometry but only put an upper limit. On the other hand, the circumstance that with both metallicities we obtain the same age and distance modulus (obviously not the same reddening) emphasizes the robustness of their values.

Of the Padova models we used the ones with $Z = 0.004$ and 0.008. In the first case, we obtain the best match assuming a cluster age of 1.7 ± 0.2 Gyr, a reddening of $E(B - V) = 0.52 \pm 0.04$ and a distance modulus of $(m - M)_0 = 13.05 \pm 0.13$. Both the RC and RH levels have a good fit, matching also the RC colour. As for the FST models, we find a slightly redder MS for $V > 19$ mag. The difference remains also with the other tracks with $Z = 0.008$. For this metallicity we estimate a cluster age of 1.7 ± 0.2 Gyr, $E(B - V) = 0.44 \pm 0.04$ and a distance modulus of $(m - M)_0 = 13.10 \pm 0.13$. Moreover, for the Padova models we can put only an upper limit to the cluster metallicity using $(B - V)$ and $(V - I)$ CMDs, and constrain the metallicity estimate in terms of the best synthetic CMD fit. Again for age and distance we get stable solutions.

With the FRANEC models we used metallicity $Z = 0.006$ and 0.01. In the former case, we can match the RH and RC levels with a reasonable fit of the upper part of the MS while the lower part $(V > 18.5)$ has a redder $(B - V)$ colour. We determine a cluster age

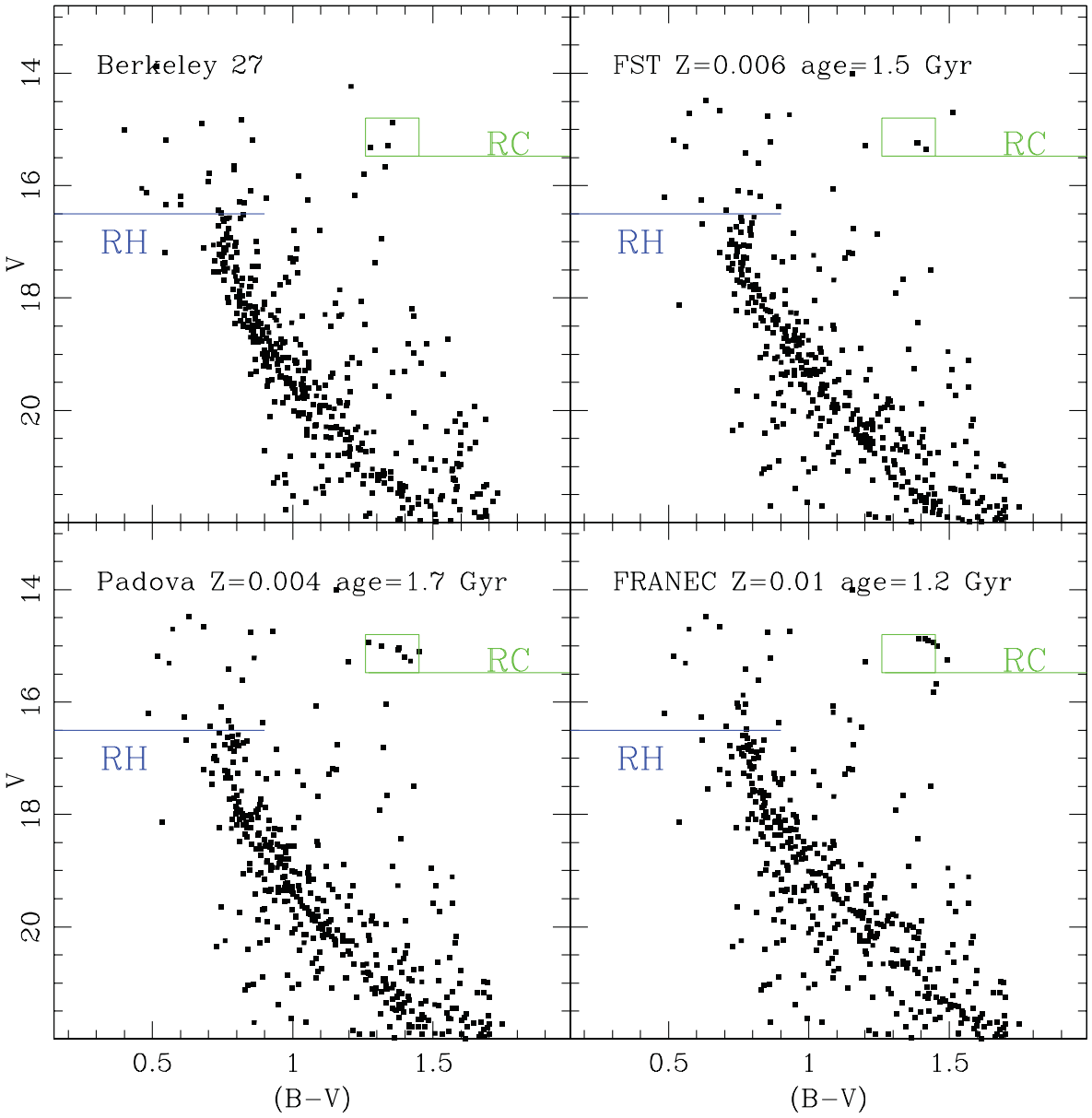

Figure 11. Top-left panel: CMD of stars inside 2.2 arcmin radius area of Be 27. The top-right panel shows the best-fitting CMD obtained with FST model: $Z = 0.006$, age 1.5 Gyr, $E(B - V) = 0.50$ and $(m - M)_0 = 13.2$; the bottom-left panel is the synthetic CMD obtained with Padova track: $Z = 0.004$, age 1.7 Gyr, $E(B - V) = 0.52$ and $(m - M)_0 = 13.05$; finally, in the bottom-right panel the CMD has been obtained with the FRANEC model: $Z = 0.01$, age 1.2 Gyr, $E(B - V) = 0.50$ and $(m - M)_0 = 13.1$.

of 1.2 ± 0.2 Gyr, $E(B - V) = 0.54 \pm 0.04$ and $(m - M)_0 = 13.1 \pm 0.13$. For the latter case, we obtain a fit that shares the same problems as the previous one: the RH and RC levels are well matched but the lower part of the synthetic MS is redder for $V > 18.5$. Accepting these differences we confirm a cluster age of 1.2 ± 0.2 Gyr with $E(B - V) = 0.50 \pm 0.04$ and $(m - M)_0 = 13.10 \pm 0.13$. For the FRANEC models the higher metallicity ($Z = 0.01$) gives a slightly better match both in $(B - V)$ and $(V - I)$, reproducing the RH phase better. As usual, the ages derived from the FRANEC models are lower than those from both the Padova and the FST ones. This is because the FRANEC tracks do not include overshooting from convective cores, while the other two sets do.

Fig. 11 shows the comparison between the observed CMD (top-left) and the best fits obtained with the three sets of tracks.

From this analysis, it turns out that the FST models are the ones that best fit the observed CMD as they provide a better match of the MS shape. This restricts the age to 1.5 Gyr. Consequently, the Galactic reddening is between 0.40 and 0.50 mag which nicely compares with the Schlegel, Finkbeiner & Davis (1998) estimate of 0.49 mag, while the distance modulus is between 13.2 and 13.3.

Carraro & Costa (2007) assign an age of 2 Gyr to Be 27, which is older than our estimates but still compatible with the results obtained with the Padova models (the ones used by the authors). This difference is mainly due to the identification of the RC level. The cluster in fact lacks a clear RGB and clump, leaving more uncertainties on the age determination. Restricting the comparison to the Padova models, the chosen metallicity used for the fit can explain the difference in the reddening estimate, as the photometry

offset between our data and theirs is of the order of 0.03 mag for $(V - I)$: for higher metallicities the fit requires lower reddening values as the isochrone has a redder colour. We find a larger distance modulus (about 0.4 mag) and this is mainly due to the age adopted (the offset in photometry is only of the order of 0.05 mag): the higher the age the fainter the magnitude of the TO; therefore, a good fit is obtained with a smaller value of the distance modulus.

4.2 Berkeley 34

The CMD of Be 34 is much richer than that of Be 27. In Fig. 12 we show the $(B - V)$ and $(V - I)$ CMDs for different circular areas centred on the cluster. The plots on the left are a selection of the very central part of Be 34 (distance r lower than 0.8 arcmin): the MS is well visible and we indicate the RH level, positioned near $V = 18.5$ mag, and the MSTP level, set near $V \sim 18.0$ mag. In the central ($r < 1.5$ arcmin) and right-hand ($r < 2.5$ arcmin) panels the MS is better delineated but with a heavier contamination of field stars. We identify two different equally probable locations for the RC: one is the bright small group of three stars at $V \sim 15.7$ mag and $(B - V) \sim 1.7$ (dashed arrow on the right), the second is the fainter group (four and more sparse stars) at $V \sim 16.7$ and $(B - V) \sim 1.55$ (solid arrow on the right). The uncertainty on the RC level comes from the fact that this evolutionary phase is very scarcely populated. In the first case, we would estimate an older age for the cluster, as the magnitude difference between the MSTP and the RC levels is larger.

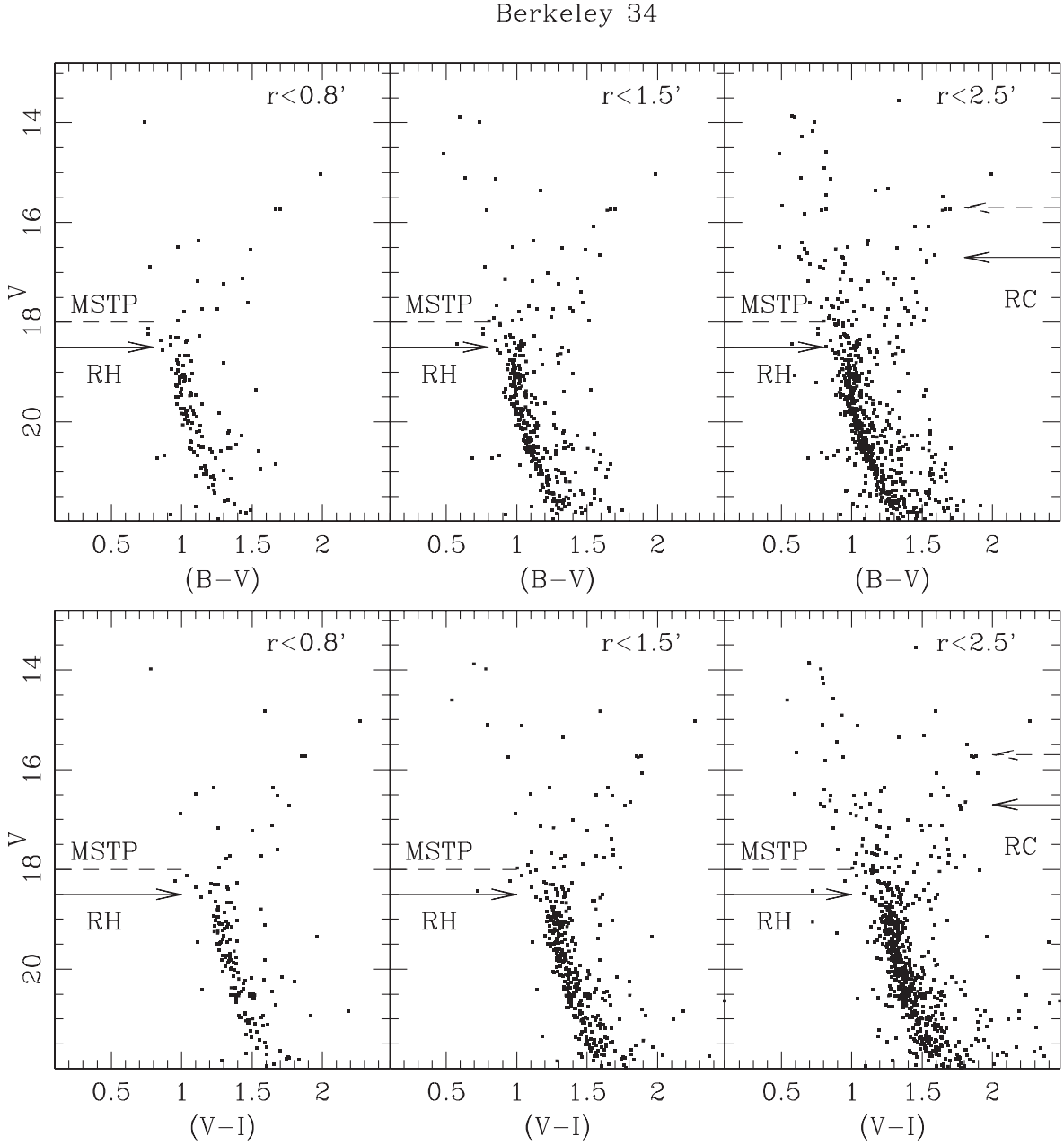

Figure 12. Upper panels show the V versus $(B - V)$ CMDs of Be 34 for different distances r from the cluster centre. Lower panels show the same but for the V versus $(V - I)$ CMDs. The levels of RH (solid arrow on the left) and MSTP (dashed line) are also indicated in the plots. We indicate also the two RC levels identified: dashed (rejected) and solid (adopted) arrows on the right.

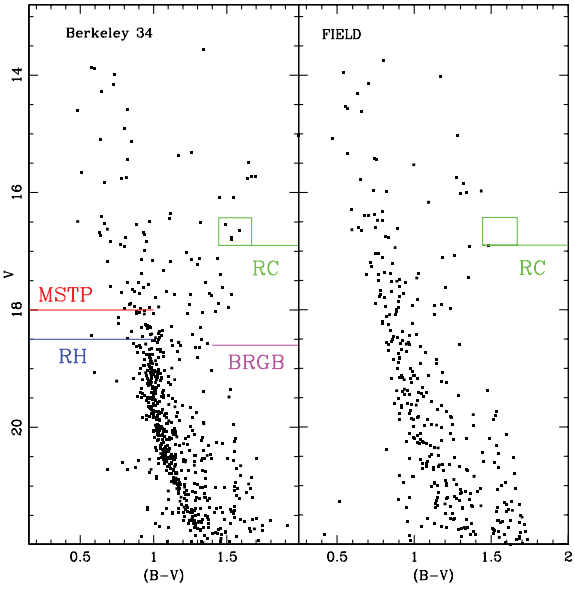

Figure 13. Left-hand panel: CMD of Be 34 for stars falling inside a region of 2.5 arcmin from the cluster centre. We indicate the luminosity level of the RH, the MSTP, the RC and the BRGB. Right-hand panel: CMD of the comparison field of an equal area.

In Fig. 12 we show, in the left-hand panel, the CMD of stars selected in a region within 2.5 arcmin from the cluster centre (we used this selection for the following analysis) and in the right-hand panel the comparison field of an equal area. We indicate also the RH, MSTP and RC magnitude levels. The RGB is difficult to recognize. It is populated by a little bunch of stars that runs redward of $(B-V)=1.5$ and is brighter than $V=18.0$. We identify the BRGB at level $V=18.6$ (see Fig. 13). In the comparison field there is no star with $(B-V)>1.5$ and no counterpart at the RC levels defined above.

As for Be 27, the MS appears broader than expected from the photometric errors: presumably differential reddening and binaries play a non-negligible role in shaping the MS appearance. For our simulations we considered a differential reddening of at least 0.05 mag. The percentage of binaries was computed using the same approach as for Be 27, finding an average fraction of 27 per cent.

In order to put limits on the cluster age and metallicity, the CMD of the region within 2.5 arcmin is compared with our synthetic CMDs. We found that models with metallicity $Z<0.02$ are in agreement with both $(B-V)$ and $(V-I)$; therefore we discarded models with solar metallicity.

If we adopt the brighter RC level estimation we find that the synthetic CMDs can match well the indicators' levels (RH, MSTP and RC) but with a worse fit for the lower MS ($V>18.0$) and for the RGB and RC colours (too blue). Even if the colour indicators are prone to greater uncertainties, as explained at the beginning of this section, in our opinion these discrepancies come from an incorrect age estimation: as the age of the stellar population increases the colour extension of the subgiant branch (SGB) becomes shorter. We thus took this age-sensitive indicator also into account, looking for a reasonable match of the distance in colour between the MS and the BRGB. In addition, these solutions cannot fit the very bright $(V\sim15)$ and red $(B-V\sim2.0)$ star, which seems to be an RGB cluster member. Our final choice is therefore to identify the RC at $V\sim17.2$ and $(B-V)\sim1.55$.

For the FST models (with overshooting parameter $\eta=0.2$) we find a reasonable agreement between synthetic and observed CMDs for a cluster age of 2.1 ± 0.2 Gyr with both metallicities $Z=0.006$ and 0.01. The RH, MSTP, BRGB and RC levels are well matched with a proper fit of the MS and the RGB shapes. The better match is obtained with the model with $Z=0.01$: the bright red member mentioned above suggests an RGB inclination that better matches the metal-rich model. The chosen binary fraction seems to be in agreement with the observations: the broad lower part of the MS is well reproduced. The reddening and distance modulus assigned for the model with $Z=0.006$ are $E(B-V)=0.62\pm0.04$ and $(m-M)_0=14.2\pm0.13$. For $Z=0.01$ we estimated $E(B-V)=0.57\pm0.04$ and $(m-M)_0=14.3\pm0.13$. From this analysis, we find that the models with $Z=0.006$ and 0.01 provide good matches both in the $(B-V)$ and $(V-I)$ CMDs, leaving the choice between these two metallicities open.

Using the Padova tracks with $Z=0.004$ and 0.008 we obtain in both cases a good match for RH, MSTP and BRGB magnitudes and colours, as well as a reasonable fit for the MS shape and RGB colour and inclination. Also in this case, the best match is obtained using the metal-richer model. For $Z=0.004$ we infer a cluster age of 2.5 ± 0.2 Gyr, $E(B-V)=0.64\pm0.04$ and a distance modulus of $(m-M)_0=14.1\pm0.13$. With $Z=0.008$ we derive a cluster age of 2.3 ± 0.2 Gyr, $E(B-V)=0.59\pm0.04$ and a distance modulus of $(m-M)_0=14.2\pm0.13$. Also for the Padova models with subsolar metallicity we obtain a good match in the $(B-V)$ and $(V-I)$ CMDs, hence we cannot firmly choose between $Z=0.004$ and 0.008.

With the FRANEC models we obtain a younger age estimate for the cluster. These models in fact do not consider overshooting and this naturally leads to a lower age prediction. The younger age required to fit the luminosity constraints results in a synthetic CMD that has a too red RGB and a too faint BRGB. For $Z=0.006$ we estimate a cluster age of 1.6 ± 0.2 Gyr, $E(B-V)=0.67\pm0.04$ and a distance modulus of $(m-M)_0=14.2\pm0.13$. With $Z=0.01$ we obtain a cluster age of 1.6 ± 0.2 Gyr, $E(B-V)=0.65\pm0.04$ and a distance modulus of $(m-M)_0=14.2\pm0.13$. In this case the higher metallicity ($Z=0.01$) gives a slightly better match both in $(B-V)$ and $(V-I)$, with a better fit of the upper MS morphology.

Fig. 14 shows the best-fitting CMD for each set of tracks and the corresponding parameters. We prefer the FST models as they give a better description of the CMD morphology as a whole. In fact we find that the Padova models predict an MS shape too curved before the RH point. The FRANEC models, instead, give a good match of the magnitude indicators but a worse fit for the MS shape and RGB inclination. With this assumption the age of Be 34 is estimated as 2.1 Gyr, with a range in reddening between 0.57 and 0.62 (similar to the Schlegel et al. 1998 value of 0.68)[6] and a distance modulus between 14.2 and 14.3.

Ortolani et al. (2005) assign to this cluster an age of 2.3 Gyr, which is in agreement with our estimation. In particular, it coincides with the one we obtained with the Padova models (the ones used by them). However, their choice of the RC level does not seem to agree with either one of our two possibilities. A non-negligible difference is found in the reddening and distance modulus determination. In the first case the discrepancy can be explained in terms

[6] Unfortunately, given the very low latitude of all three OCs, these reddening values cannot be trusted to give the real asymptotic reddening, and they cannot give a firm constraint as in more favourable cases.

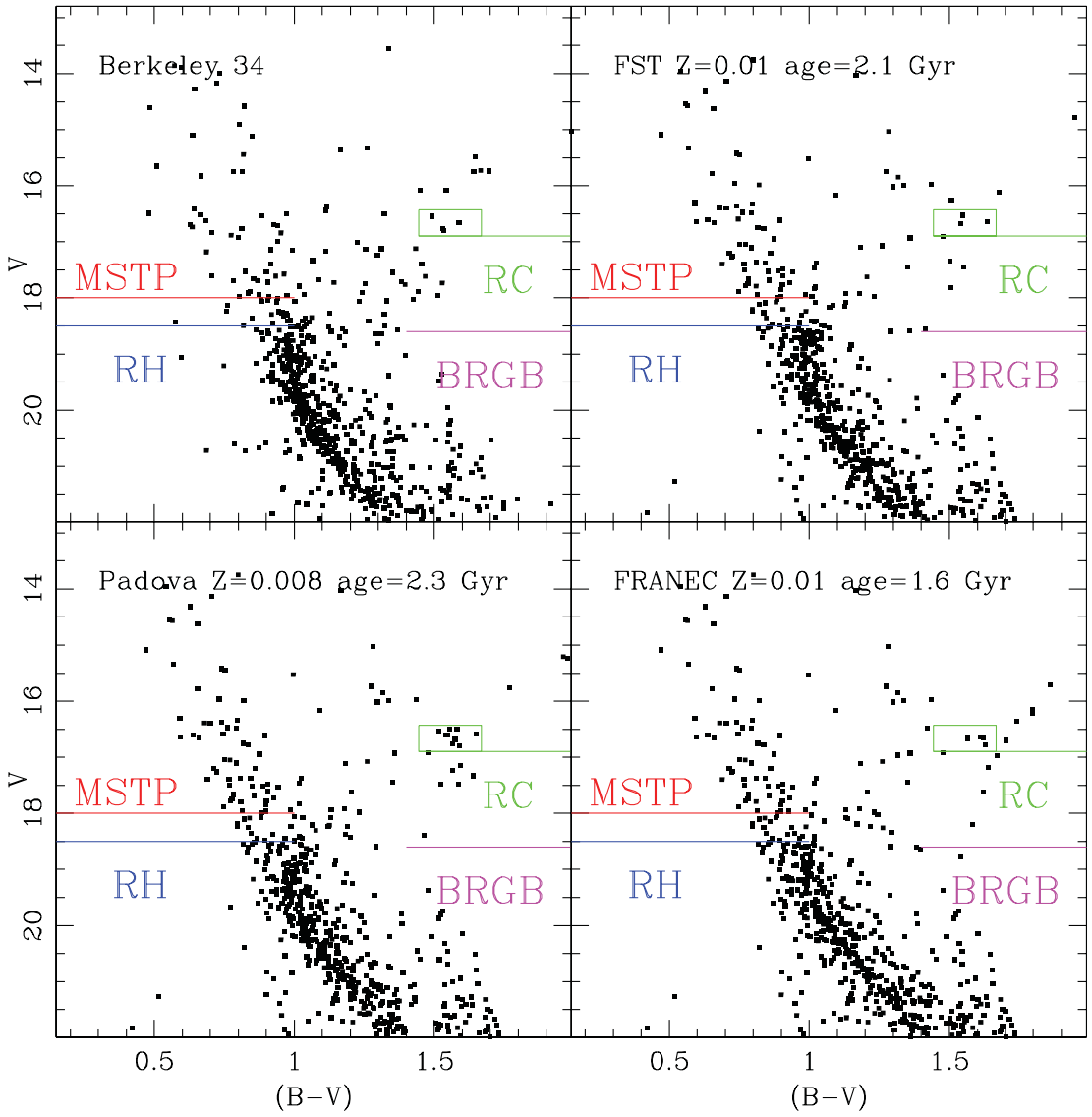

Figure 14. Top-left panel: CMD of stars inside 2.5 arcmin radius area of Be 34. The top-right panel shows the best-fitting CMD obtained with the FST model: $Z = 0.01$, age 2.1 Gyr, $E(B-V) = 0.57$ and $(m-M)_0 = 14.3$; the bottom-left panel is the synthetic CMD obtained with the Padova track: $Z = 0.008$, age 2.3 Gyr, $E(B-V) = 0.59$ and $(m-M)_0 = 14.2$; finally, in the bottom-right panel the CMD has been obtained with the FRANEC model: $Z = 0.01$, age 1.6 Gyr, $E(B-V) = 0.65$ and $(m-M)_0 = 14.2$.

of differences between our photometries (see Section 2.4). For the distance modulus the differences in the photometries cannot explain such discrepancy: we note that they choose an MSTP level of about half a magnitude brighter with respect to our analysis, hence they determine a smaller distance modulus.

4.3 Berkeley 36

Be 36 is the richest cluster of the group. The CMDs in Fig. 15 clearly show the MS, the MSTP ($V \sim 18.1$) and the RGB for different distances from the cluster centre. The contamination from field stars is evident particularly in the central and right-hand panel: the MS is blurred and the region above the MSTP is dominated by field interlopers (together with the cluster blue straggler stars, very common in OCs, see e.g. Ahumada & Lapasset 2007, for a recent catalogue). Moreover, for this cluster we restricted our analysis to a small area of radius 2.3 arcmin to maximize the membership likelihood. Even within this restricted area we can still note an important field contamination but without losing the evidence of the CMD features: the MSTP at $V \sim 18.1$ and the BRGB at the magnitude level of $V \sim 18.6$ (see Fig. 16). We also note a small gap at $V \sim 18.7$ which could be associated with an RH phase; however, further investigations discarded this hypothesis. The RGB is quite evident, running redward of $(B-V) = 1.5$ and reaching $V \sim 14.5$ with a very red member at $B-V \sim 2.2$. The field contamination along the RGB seems very modest, from comparison to an equal area of the external field (Fig. 16). Yet, the RC level is not so evident: we adopted as RC the small group of stars (two) located at $V \sim 16.0$ (in Fig. 15 we indicate the probable RC with the dashed arrow). However, even though we obtained a good fit of the RC and MSTP levels and of the MS shape, we could not obtain a good description of the RGB phase, too red in the synthetic CMDs. This is due to a too extended SGB phase, suggesting that we are adopting too young an age for the cluster. To help choose the best solution even without

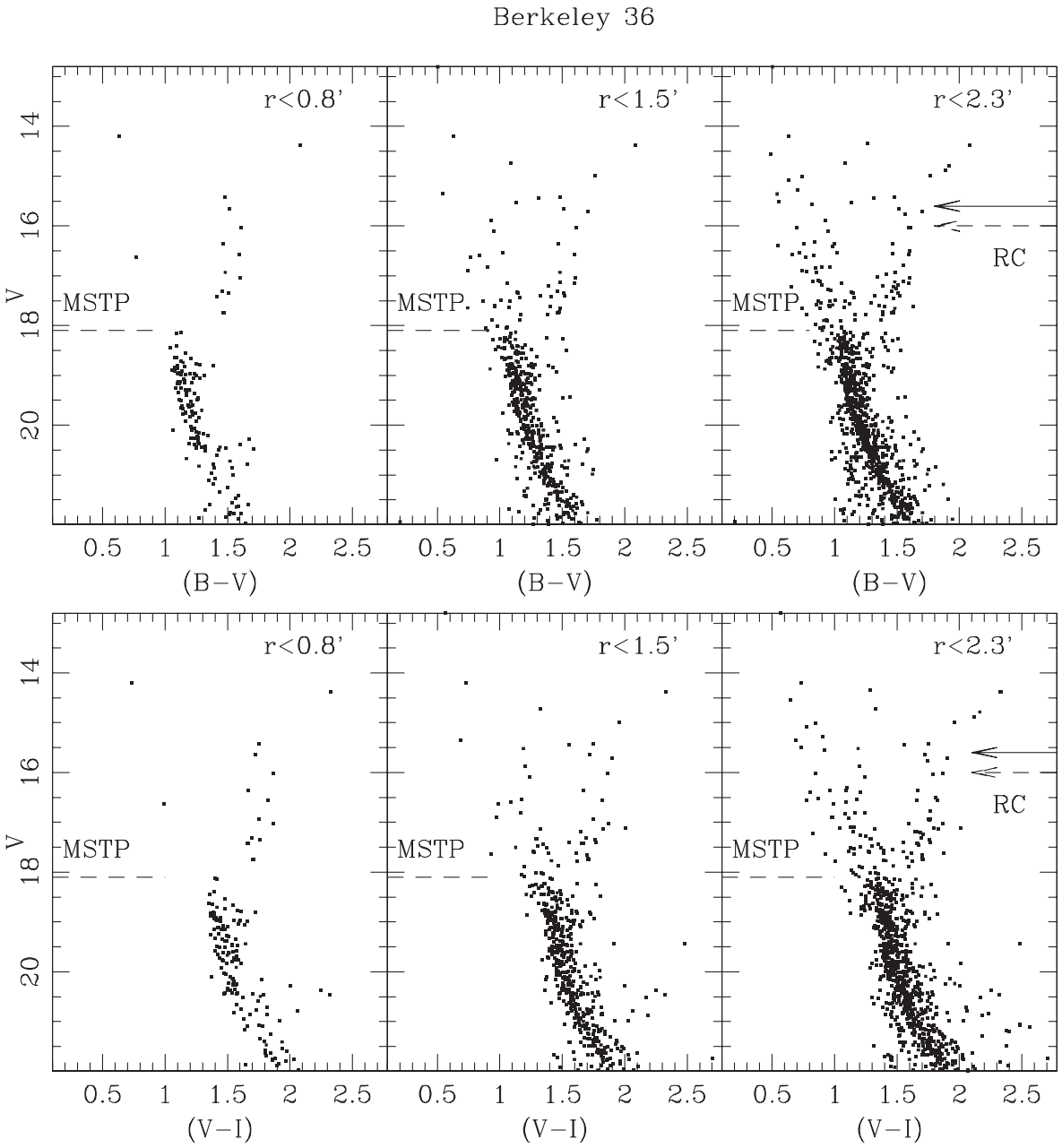

Figure 15. Upper panels show the V versus $(B - V)$ CMDs of Be 36 for different distances r from the cluster centre. Lower panels show the same but for the V versus $(V - I)$ CMDs. In the plots we indicate the levels of MSTP (dashed line) and RC. The dashed arrow is for the rejected level (see the text) and the solid arrow is for the adopted RC level.

firm evidence of the RC stars, we compared the CMD of Be 36 with those of two of the oldest clusters inside the BOCCE project: Be 17 and Be 32. Be 17 is among the oldest OCs of the Galaxy, with an age in the range 8.5–9.0 Gyr (Bragaglia et al. 2006) while Be 32 is 5–5.5 Gyr old (Tosi et al. 2007). They both have subsolar metallicity, as expected for Be 36 from previous analysis.

In Fig. 17 we show a comparison of the CMDs of Be 32, Be 36 and Be 17. In the left- and right-hand panels we present the CMDs of Be 32 and Be 17 using absolute magnitude M_V and intrinsic colour $(B - V)_0$. We used different limits on the magnitude (y-axis) to visually align the luminosity level of the evolutionary MSTP phase of the clusters, preserving the magnitude and colour range in order to properly compare the CMDs. We also show the isochrones which best fit the clusters according to our analysis (dashed line for Be 32 and solid line for Be 17). We overplot them on the CMD of Be 36 after a proper alignment in colour and magnitude. While both isochrones fit well the upper and lower MS, they bracket the RGB of Be 36 on the red and blue sides.

This indicates that Be 36 is in an evolutionary status, an intermediate between that of Be 32 and Be 17. In particular, we can discard a cluster age younger than about 5 Gyr, as it would imply a more extended SGB and a redder RGB, while the older isochrone shown in the comparison sets a upper limit (8.5 Gyr) to the cluster age. Assuming the ages of Be 32 and Be 17 as limits for Be 36, the corresponding most probable RC locus for this cluster is at $V \sim 15.5$ and $(B - V) \sim 1.55$ (solid arrow on the right in Fig. 15).

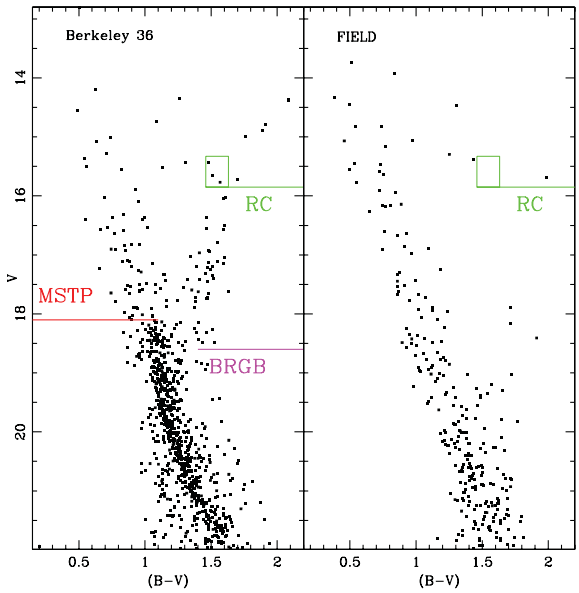

Figure 16. Left-hand panel: CMD of Be 36 for stars falling inside a region of 2.3 arcmin from the cluster centre. We indicate the luminosity level of the MSTP, BRGB and the RC. Right-hand panel: CMD of an equal area of the comparison field.

The three stars enclosed in the box in Fig. 16 are very few but likely to be cluster members as they are positioned near the cluster centre.

Having decided the RC position and an age range, we applied the usual method of analysis, taking into account the very scattered characteristic of the CMD. We adopted a higher differential reddening of 0.15, the only viable solution to reproduce the MS spread, and a binary fraction of 25 per cent. Given the more scattered appearance, these values have larger uncertainties than for the two other clusters. Keeping these parameters fixed we investigated the possibility to fit simultaneously the MSTP, BRGB and RC luminosities by adjusting the age, the mean Galactic reddening and the distance modulus.

Moreover, for Be 36 we restricted our analysis to models with subsolar metallicity: a metallicity of $Z = 0.02$ cannot match at the same time $B - V$ and $V - I$, predicting an RGB with a strong inclination in the upper part. In contrast with what was found for Be 27 and Be 34, all the explored models predict a lower MS slightly bluer than observed. We could not use the FRANEC models as they have incomplete evolutionary tracks for ages older than 5 Gyr for subsolar metallicities. Fig. 18 displays the best-fitting CMD for each set of tracks compared with the observational CMD (upper panel).

The FST models can reproduce quite well the magnitudes and colours of the indicators, even though they predict a bluer MS for $V > 21$. We find a better match for models with $Z = 0.006$. For $Z = 0.01$, when the synthetic $B - V$ CMD is correct, the $V - I$ always turns out slightly bluer than observed. The best solution is obtained for the models with $Z = 0.006$, a cluster age of 7.0 ± 1.0 Gyr, a mean reddening of $E(B - V) = 0.53 \pm 0.04$ and a distance modulus of $(m - M)_0 = 13.15 \pm 0.13$. For $Z = 0.01$ we find the same age of 7.0 ± 1.0 Gyr, $E(B - V) = 0.48 \pm 0.04$ and $(m - M)_0 = 13.19 \pm 0.08$.

Using the Padova models we find a good match for the MSTP, BRGB and RC levels with a better description of the MS (bluer only for $V > 21.5$). The best matches are obtained with models with $Z = 0.008$, when the synthetic CMDs can match the observed one both in $B - V$ an $V - I$ at the same time. We find a cluster age of 7.5 ± 1.0 Gyr, $E(B - V) = 0.51 \pm 0.04$ and $(m - M)_0 = 13.1 \pm 0.13$; the synthetic CMD obtained with these parameters reproduces the MS and RGB shape and colour quite well, even if it cannot reproduce correctly the overdensity observed at $V \sim 17$ along the RGB.

The comparison with previous results (Ortolani et al. 2005) shows a significant discrepancy in the cluster age and therefore in the determination of cluster reddening and observed distance modulus. This is due in part to the choice of the MSTP level and in part to the disagreement in the photometries (see Section 2.4). Concerning the age they set the MSTP level at half a magnitude brighter than our estimation, adopting the same RC level we use for the analysis. This implies a younger age and a smaller distance modulus estimations. The difference in the reddening estimates is mainly due to the remarkable disagreement in the photometries.

5 CONCLUSIONS

The purpose of this paper is to add additional empirical information to the models of the Galactic disc structure and chemical evolution. We studied three distant OCs towards the anticentre direction using SUSI2/NTT *BVI* photometry. With these data we obtained CMDs 1 mag deeper with respect to the ones found in the literature. This aspect is especially relevant for the more distant and reddened clusters Be 34 and Be 36, for which we could obtain more precise data for the lower MS. The analysis was carried out using the synthetic CMD technique that allowed us to infer a confidence interval for age, metallicity, binary fraction, reddening and distance for each cluster. We used three different sets of stellar tracks (Padova, FST and FRANEC) to describe the evolutionary status of the clusters in order to minimize the model dependence of our analysis. We found the following.

(i) Be 27 is located at about 4.0–4.5 kpc from the Sun [assuming the normal extinction law $R_V = A_V/E(B - V) = 3.2$]. Its position in the Galactic disc is at $R_{GC} \sim 11.8$–12.2 kpc and 185–205 pc above the plane (assuming $R_\odot = 8$ kpc as in our previous works). The resulting age varies between 1.2 and 1.7 Gyr, depending on the adopted stellar model, with better fits for ages between 1.5 and 1.7 Gyr. A metallicity lower than the solar value seems preferable. The mean Galactic reddening $E(B - V)$ is between 0.44 and 0.54 and we estimate a (lower limit) fraction of binaries of about 25 per cent.

(ii) Be 34 is 6–7 kpc away from the Sun, with a distance from the Galactic Centre of about 14.0–14.6 kpc and located 220–240 pc above the plane. The age is between 1.5 and 2.5 Gyr, with better fits in the age range 2.1–2.5 Gyr. The metallicity for this cluster is lower than the solar value; the mean Galactic reddening $E(B - V)$ is between 0.57 and 0.64. The estimated binary fraction for this cluster is about 27 per cent.

(iii) Be 36 is about 4.2 kpc away from the Sun. Its distance from the Galactic Centre is $R_{GC} \sim 11.3$ kpc and it lies 40 pc below the plane. This cluster shows a broad differential reddening up to +0.15, adding uncertainty to the interpretation of the cluster parameters. The best-fitting age is between 7.0 and 7.5 Gyr with a preference for models with a metallicity lower than the solar value and higher than $Z = 0.004$. The reddening estimate is $E(B - V) \sim 0.5$, while the binary fraction is of the order of 25 per cent.

Poorly populated clusters such as Be 27 have a very loose and barely observable RC and RGB, a condition that adds uncertainties to the study of the evolutionary status of the objects. On the other hand, clusters such as Be 34 and Be 36 have a much more significant RGB

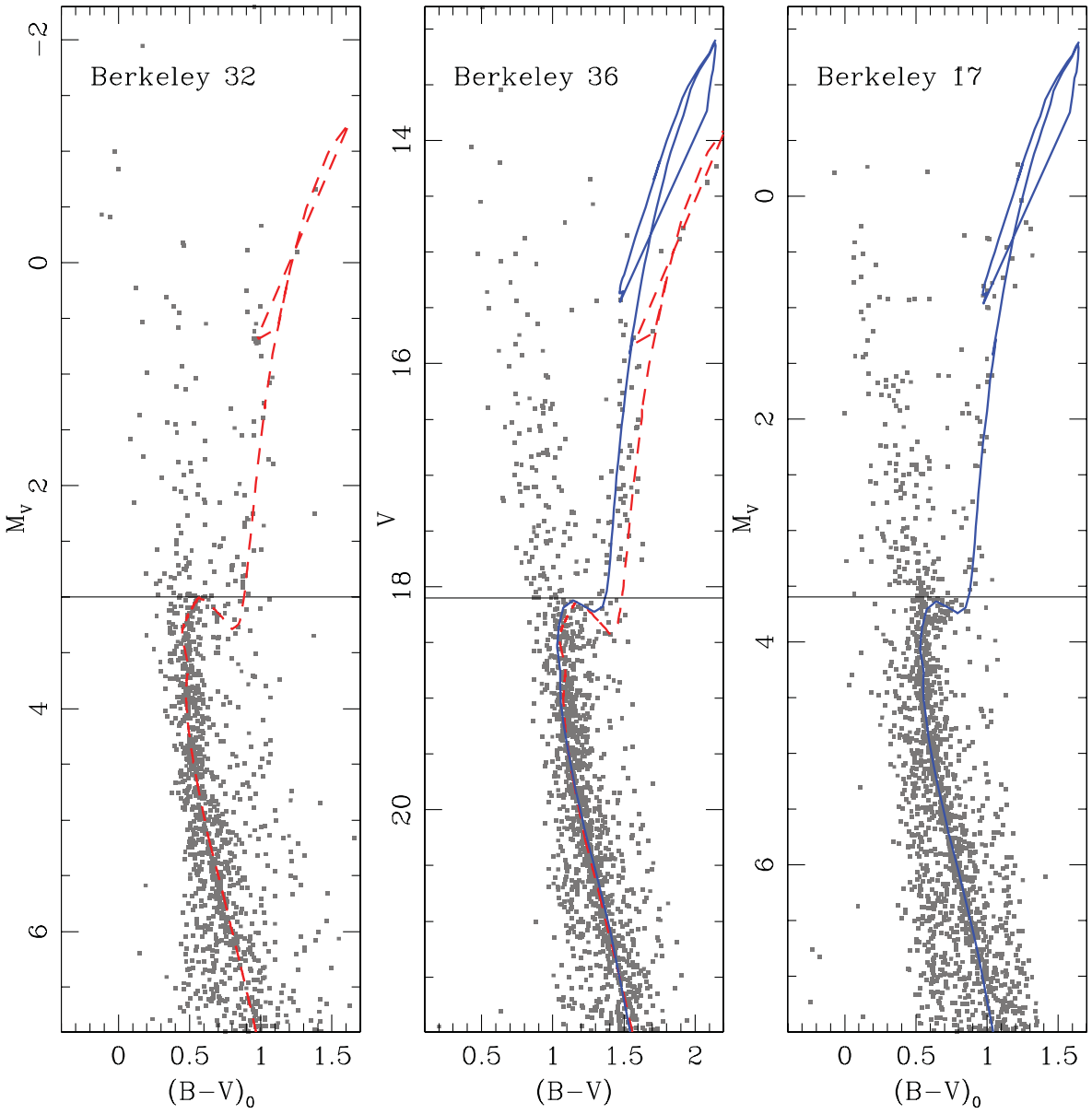

Figure 17. Left-hand panel: CMD M_V, $(B-V)_0$ of Be 32. The dashed line is the best-fitting solution described in Tosi et al. (2007): $Z = 0.008$, age 5.2 Gyr, $E(B-V) = 0.12$ and $(m-M)_0 = 12.6$ for the Padova models. Central panel: CMD of Be 36 with the overplot of the best-fitting isochrones of Be 32 (dashed line) and Be 17 (solid line). Right-hand panel: CMD M_V, $(B-V)_0$ of Be 17. The solid line is the best-fitting solution for the Padova models described in Bragaglia et al. (2006): $Z = 0.008$, age 8.5 Gyr, $E(B-V) = 0.62$ and $(m-M)_0 = 12.2$. We used different limits on the magnitude (y-axis) for the three plots in order to visually align the evolutionary MSTP phase of the clusters but preserving the magnitude and colour range for an easier comparison. The solid horizontal lines set the MSTP level.

but suffer from a greater contamination of field stars and a stronger differential reddening: in this case the RC determination is strongly affected by these two aspects. Relaxing the assumptions on the RC position could noticeably change the cluster age for Be 27, for which we can only rely on the MSTP and MS shape, while for Be 34 and Be 36, the additional information on the well-populated RGB better constrains the analysis. A robust determination of the parameters of the three clusters would require additional information on cluster membership for evolved and main-sequence turn-off stars. This is obtainable in the immediate future by measuring radial velocities of at least many tens of stars, or we can wait for the results of the *Gaia* astrometric satellite, with precise individual distances and proper motions.

For all the three clusters we found a metallicity lower than the solar value, even if we were not able to unambiguously tell if $Z = 0.004$, 0.006, 0.008 or 0.01 (depending on the track used) is to be preferred. This conforms to their Galactocentric distance. Only high-resolution spectroscopy of these clusters will be able to definitely determine the metallicity value. Given the relatively faint magnitudes even of the red giants, an 8–10 m telescope will be necessary; it is however an important piece of information for the chemical modelling of the Galaxy.

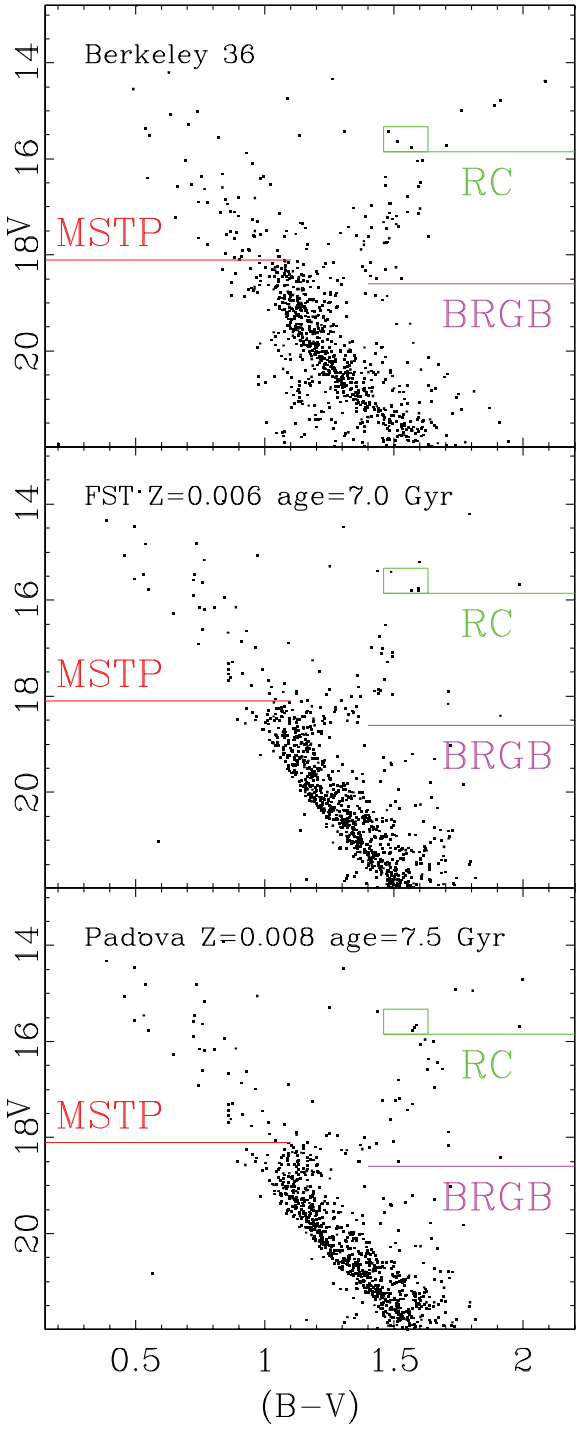

Figure 18. Top panel: CMD of stars inside 2.3 arcmin radius area of Be 36. The central panel shows the best-fitting CMD obtained with the FST models: $Z = 0.006$, age 7.0 Gyr, $E(B - V) = 0.53$ and $(m - M)_0 = 13.15$; the bottom panel is the synthetic CMD obtained with the Padova tracks: $Z = 0.008$, age 7.5 Gyr, $E(B - V) = 0.51$ and $(m - M)_0 = 13.1$.

ACKNOWLEDGMENTS

We thank Paolo Montegriffo for providing the software for catalogue matching, which we used consistently in this work. We are grateful to the referee, Bruce Twarog, for his encouraging and always constructive comments. This research has made use of the WEBDA data base, operated at the Institute for Astronomy of the University of Vienna, the VizieR catalogue access tool (CDS, Strasbourg, France) and NASA's Astrophysics Data System.

REFERENCES

Ahumada J. A., Lapasset E., 2007, A&A, 463, 789
Andreuzzi G., Bragaglia A., Tosi M., Marconi G., 2011, MNRAS, 412, 1265
Bellazzini M., Fusi Pecci F., Messineo M., Monaco L., Rood R. T., 2002, AJ, 123, 1509
Bragaglia A., Tosi M., 2006, AJ, 131, 1544
Bragaglia A., Tosi M., Andreuzzi G., Marconi G., 2006, MNRAS, 368, 1971
Bressan A., Fagotto F., Bertelli G., Chiosi C., 1993, A&AS, 100, 647
Carraro G., Costa E., 2007, A&A, 464, 573
Cignoni M., Beccari G., Bragaglia A., Tosi M., 2011, MNRAS, 416, 1077
Dean J. F., Warren P. R., Cousins A. W. J., 1978, MNRAS, 183, 569
Dias W. S., Alessi B. S., Moitinho A., Lépine J. R. D., 2002, A&A, 389, 871
Dominguez I., Chieffi A., Limongi M., Straniero O., 1999, ApJ, 524, 226
Friel E. D., 1995, ARA&A, 33, 381
Friel E. D., Jacobson H. R., Pilachowski C. A., 2010, AJ, 139, 1942
Hasegawa T., Malasan H. L., Kawakita H., Obayashi H., Kurabayashi T., Nakai T., Hyakkai M., Arimoto N., 2004, PASJ, 56, 295
Landolt A. U., 1992, AJ, 104, 340
Lépine J. R. D. et al., 2011, MNRAS, 417, 698
Ortolani S., Bica E., Barbuy B., Zoccali M., 2005, A&A, 439, 1135
Schlegel D. J., Finkbeiner D. P., Davis M., 1998, ApJ, 500, 525
Sestito P., Bragaglia A., Randich S., Pallavicini R., Andrievsky S. M., Korotin S. A., 2008, A&A, 488, 943
Stetson P. B., 1987, PASP, 99, 191
Stetson P. B., 1994, PASP, 106, 250
Tosi M., Bragaglia A., Cignoni M., 2007, MNRAS, 378, 730
Ventura P., Zeppieri A., Mazzitelli I., D'Antona F., 1998, A&A, 334, 953

This paper has been typeset from a TEX/LATEX file prepared by the author.